Izvorni znanstveni rad/Original scientific paper

Fourier vs. wavelet analysis: the case of the Adriatic Sea Surface Temperature

Milivoj Kuzmić[1] *and* ***Zoran Pasarić***[2]

Primljeno/Received: 12. 12. 2003
Prihvaćeno/Accepted: 04. 04. 2007

[1]*Centre for Marine and Environmental Research*
Rudjer Bosković Institute
P.O. Box 180, 10002 Zagreb
E-mail: kuzmic@rudjer.irb.hr

[2]*Geophysical Department, Faculty of Science*
Horvatovac bb, 10000 Zagreb
E-mail: pasaric@rudjer.irb.hr

ABSTRACT – In this paper, we compare two approaches (Fourier and wavelet) to the spectral analysis of time series, using five-day averaged maps of the remotely sensed Adriatic Sea surface temperature (SST) as an example. Both analyses have been performed in conjunction with the empirical orthogonal function (EOF) analysis of the surface temperature fields. The Fourier power spectra of the first EOF mode (the dominant part of the overall signal, used to assess the difference between the approaches) were calculated using the Welch averaged periodogram. The Morlet mother wavelet was used in calculating the continuous wavelet transform (CWT). By using the CWT we were able to decompose the one-dimensional time series of the Adriatic SST variability into a two-dimensional time-frequency space, discerning the series` dominant modes of variability as well as changes in those modes over a 14-year period (1985-1998). The Fourier analysis singled out important, but by definition global, periodicities uniformly spanning the whole analysed period. In contrast, the wavelet analysis, besides annual and semi-annual harmonics, offered a plenitude of other periods, with modal intensities changing in time.

Keywords: Fourier analysis, wavelet transform, the Adriatic, sea surface temperature

SAŽETAK – U ovom se radu, na jadranskom primjeru petodnevno usrednjenih polja daljinski detektirane površinske temperature mora (PTM), uspoređuju dva pristupa spektralnoj dekompoziciji vremenskih nizova (putem Fourierove te valične analize). Obje analize su provedene na temelju površinskih temperaturnih polja prethodno razloženih uporabom empirijskih ortogonalnih funkcija (EOF). Fourierovski spektri snage prvog EOF moda (dominantni dijelovi ukupnog temperaturnog signala rabljenog u usporedbi dvaju pristupa) računati su uporabom Welchovog usrednjenog periodograma. Morletov primarni valić rabljen je pri računanju kontinuirane valične transformacije (KWT). Uporabom KWT bilo je moguće razložiti jednodimenzionalni vremenski niz jadranskih PTM u

dvodimenzionalno vremensko-frekvencijsko polje, razlučujući pri tom dominantne modove temperaturne promjenjivosti kao i mijene tih modova tijekom 14-godišnjeg razdoblja (1985-1998). Fourierovom analizom izdvojene su važne, no po definiciji globalne, periodičnosti koje se uniformno javljaju tijekom čitavog analiziranog razdoblja. Nasuprot tome valična analiza je, pored godišnjeg i polu-godišnjeg harmonika, ponudila pregršt drugih periodičnosti čiji se intenzitet mijenja u vremenu.

Ključne riječi: Fourierova analiza, valična analiza, Jadran, površinska temperatura mora

1. INTRODUCTION

For decades the Fourier analysis, in its numerous implementations, has been an invaluable tool in various branches of science and engineering. Its overwhelming success in analysing time-domain signals for their frequency content has relied on Fourier's discovery that any periodic or quasi-periodic signal may be resolved into an equivalent infinite sum of sines and cosines of an increasingly higher frequency. By approximating a complex signal with a weighted sum of simpler functions the Fourier procedure may easily provide frequencies and amplitudes of the signal components, as long as infinite monochromatic basis functions are acceptable approximation. In other words, basis functions extending to infinity provide excellent frequency localization, but lose all of the temporal information.

If a signal is non-stationary, with spectral content changing in time, the frequency representation only becomes inadequate, and time-frequency expression is required instead. An immediate modification of the Fourier transform that accommodates such a request is the short-time or windowed Fourier transform (WFT). The idea of the WFT is to segment a signal in the time-domain using a finite window, and perform the classical analysis in each segment. The effect of the window is localization in time, but a drawback is the fixed window size for the entire signal duration. That is, the WFT replaces the FFT unbounded sinusoidal waves with the window-localized ones, but the constant length of the window provides the same resolution in all parts of the time-frequency plane. Consequently, a medium-length window would be too long to localize high-frequency (HF) oscillations, and too short to precisely define the low-frequency (LF) ones.

The Wavelet analysis (WA) may be viewed as an adjustable WFT that provides a better framework for dealing with the time localization. Its basis functions, the wavelets, offer localization in both time and frequency domains that narrows down on the HF oscillations and widens up to catch the LF changes. Using the WA, one is able to decompose a one-dimensional time series into two-dimensional time-frequency/scale space, and discern the series' dominant frequency modes of variability as well as changes of those modes in time. This ability makes the WA a suitable tool for the detection of episodic fluctuations of multi-scale character. Inter-annual variability in the sea-surface temperature is a

good example of such a system. Numerous books have been written on both techniques (e.g. Bloomfield, 2000 or Chui, 1997) in which one can find plenty of relevant information.

In this paper, we compare two approaches to the spectral analysis of time series (Fourier and Wavelet) using five-day averaged maps of the remotely sensed Adriatic Sea surface temperature (SST) as an example. Both analyses have been performed in conjunction with the empirical orthogonal function (EOF) analysis of the surface temperature. The paper is structured as follows: the data and processing procedures are presented next, followed by the exposition and discussion of results.

2. DATA ANALYSIS

2.1 Input data

The Adriatic Sea is an epicontinental basin with pronounced bathymetric differences and a significant freshwater inflow, connected at its Southern end to the Ionian Sea. These features decisively shape its oceanographic setting and its thermal structure in particular. The northern shallow shelf is particularly conductive to the pronounced, highly variable surface heat exchange. Winter outbreaks of cold and dry air from narrow passages between the Alpine and the Dinaric mountain chains can lead to severe wind development (Furlan, 1977). This gusty wind (bora) is known to blow from the north-eastern direction across most of the Eastern Adriatic coast, triggering over the shallow northern shelf in particular intense evaporative and heat fluxes (e.g. Hendershott and Rizzoli, 1976). On the other hand, the Po River, with its multi-annual average runoff of some 1,500 m^3/s, dominates the freshwater discharge into the basin; on the eastern side, half-as-large, a combined average runoff is provided by numerous Albanian rivers (Raicich, 1994). These processes shape the mean Adriatic temperature field whose first EOF mode is depicted in Figure 1. The figure suggests higher temperature in the middle of the basin, and colder north due to the mentioned combined effects of shallowness, continentality and freshwater exposure. The sea surface temperature of the waters along the island-rich eastern coast is not well resolved is the data, but that along the opposite coast clearly shows the combined impact of the freshwater discharges. The oceanographic aspect of this problem has been dealt with elsewhere (Kuzmić and Pasarić, 2006; in this paper we focus on the comparison between the two spectral analysis techniques.

The remotely sensed SST data set used in this study is an Adriatic subset of the NASA Seasonal to Inter-annual Project (NSIPP) Advanced High Resolution Radiometer (AVHRR) global SST set (some additional information may be found in Casey and Cornillon, 1999). It was generated using the versions 4.0, 4.1 and interim 4.1 of the NOAA/NASA Oceans Pathfinder daily averaged SST maps at 9.28 km resolution, spanning the period from 1985 to 1998. The Adriatic subset was created by extracting the area spanning 12^o–20^o East longitude, and 40^o–46^o North latitude. Consequently, there are 1022 such fields (14 years x 73 pentads /year), each consisting of 1556 pixels (areas of 9.28 x 9.28 km^2) over the Adriatic.

Each pentad map was obtained by averaging all available daily day and night Pathfinder scenes.

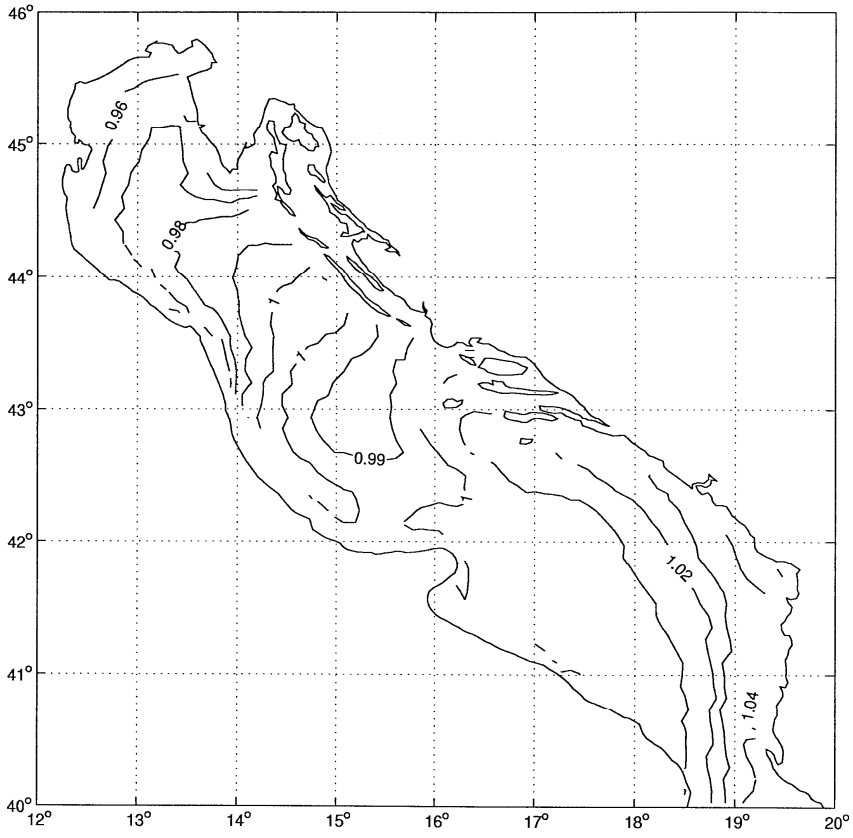

Figure 1. The first EOF mode derived from the 14-year NSIPP Adriatic SST subset.

This data set may be viewed as consisting of 1556 time series, each containing 1022 SST data values. However, these time series are hardly ever complete, due to the gaps caused by cloudy pixels. In our case, not a single time series had less than 70 gaps, and only 28 series had more than 400 gaps. The most numerous gaps were found along the Italian coast; minimal number of gaps was found in the offshore regions of the Middle and South Adriatic. The first, most obvious task was to fill in those gaps. Since we expect the annual cycle to be the most prominent part of the SST signal, the residuals were determined by subtracting an expression of the form

$a_0 + a_1\cos(\omega_1 t + \phi_1) + a_2\cos(\omega_2 t + \phi_2)$

at each pixel. Here, t is time measured in pentads, $\omega_1 = 2\pi/73$ (5 day)$^{-1}$ and $\omega_2 = 4\pi/73$ (5 day)$^{-1}$ are the annual and semi-annual frequencies, while the constants a_0, a_1, a_2, ϕ_1, ϕ_2 were determined separately by least square fit at each geographical position *(i.e.* pixel). For almost all pixels (more than 98% of them), the variance of residual fell between 3% and 5% of the total variance, and for only 3 pixels the variance exceeded 6% of the total variance. Simple linear

interpolation was then used to fill in the gaps on residuals after which the annual cycle were added back. A complete set of data was obtained in this way (both in time and space), and used in the subsequent analysis.

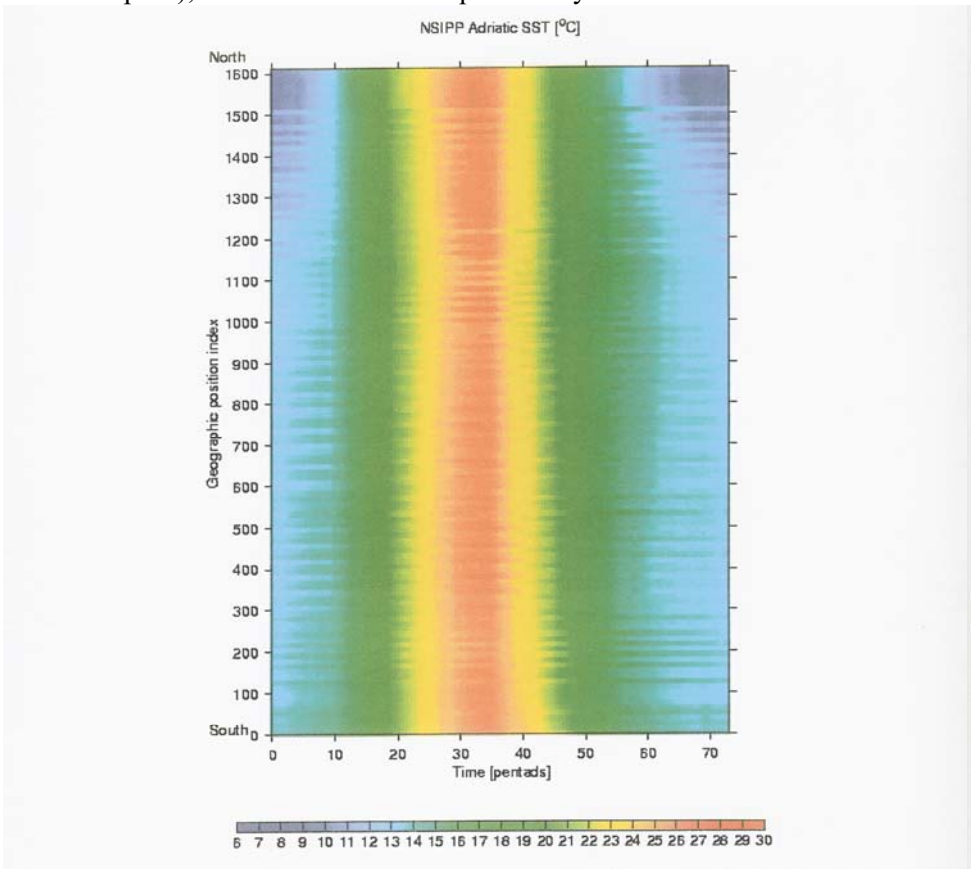

Figure 2. The Adriatic subset of the NSIPP SST climatology (1985-1998).

When 1022 pentad maps are averaged to form a perpetual year, the climatological field presented in Figure 2 is obtained. The values in the figure are sorted from the southwest (bottom) to the northeast (top). The temporal axis is shifted by 12 pentads, to start in March. One can readily observe that in winter the shallow north is climatologically colder that the deep south, whereas in summer both geographic ends attain very similar temperature. Due to the gap-filling procedure the time-versus-location Adriatic matrix is full; the observed stripes seem to be the consequence of a jump from the end of one zonal string of values (easternmost position) to the beginning of the next (westernmost position).

2.2 Data processing

As hinted in the previous paragraph, in order to obtain a time series of the Adriatic SST facilitating comparison of the Fourier and wavelet approaches, the EOF analyses were performed first, in two variants. In both cases, the covariances were calculated with respect to time. However, in the first case the EOF analysis

was done after the temporal mean had been calculated for each pixel and subtracted from the time series. In the second case, the spatial mean for each image was subtracted from that image prior to the calculation of time covariances, leading to the so-called 'gradient modes' EOF analysis. In both cases, the first mode carried a huge part of the total variance. The time components of various

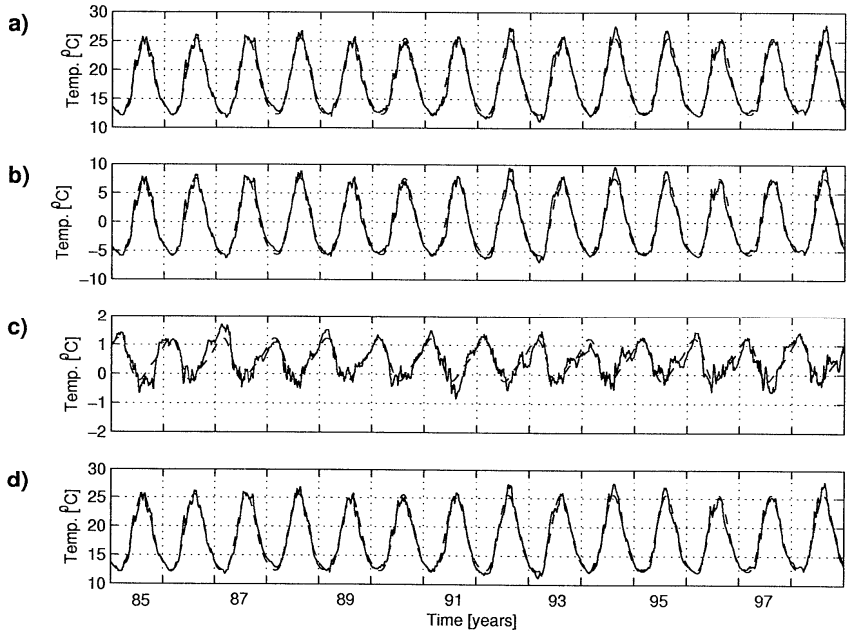

Figure 3. The time-component obtained (a) by EOF analysis of the original NSIPP data; (b) by EOF analysis of the NSIPP data after time mean is removed; (c) by EOF analysis of the NSIPP data after space mean is removed; (d) after simple spatial averaging at each time step (no EOF analysis). Also plotted in all figures are curves (dashed) obtained by fitting the data to two dominant harmonics.

analyses are displayed in Figure 3. The top series is the time component obtained by the EOF analysis of the original NSIPP data. The one below (Figure 3b) is obtained when the time mean is removed prior to the EOF analysis, and still further below is the result of prior spatial mean removal. The bottom series (Figure 3d) is the result of simple spatial averaging (no EOF analysis) at each time step. The amplitudes in Figure 3b and 3c were subsequently analyzed in more detail using the classical FFT and the CWT, succinctly exposed in the following paragraphs.

Fourier analysis

The classical power spectra of the first mode time component (for both types of the EOF analysis mentioned above) were calculated using Welch's averaged periodogram method. That is, time series were padded with 2 zeros (to obtain the length of 1024) and divided into four disjoint sections. Each section separately is multiplied by a triangular window, and the periodogram was calculated using the FFT. Finally, the four periodograms were averaged to give the power spectra.

Wavelet analysis

The CWT is a data analysis technique that transforms a signal from the one-dimensional purely time domain into the two-dimensional time-frequency domain, conveying information about the time evolution on plethora of frequency components within the signal. To apply the analysis, the so-called 'mother wavelet', or 'analyzing wavelet', has to be chosen first. It may be essentially any function $\psi(t)$ with finite energy (i.e. square-integrable) that satisfies the relation:

$$\int \psi(t)dt = 0 \text{, or } \hat{\psi}(0) = 0 \text{,}$$

where $\hat{\psi}(\varpi)$ is Fourier transform of $\psi(t)$. The mother wavelet is dilated in scale ($a > 0$) and translated by b units of time to obtain a new function (i.e. a family of functions):

$$\psi_{b,a} = \left|a^{-1/2}\right| \psi(\frac{t-b}{a}) \text{.}$$

These functions are finally used to 'measure' the contents of some frequency component (or some other property of $\psi_{b,a}$ within the signal, denoted by $x(t)$, around the time b). More precisely, the CWT is defined by the correlation:

$$(Wx)(b,a) = \int x(t)\ \overline{\psi_{b,a}\,(t-b)}dt \text{.}$$

Obviously, CWT contains a lot of redundant information, which gives detailed information on the time-scale localization, and also yields infinitely many ways to reconstruct the original signal. The simplest reconstruction formula is:

$$x(t) = C_{\psi}^{-1} \int \left|a\right|^{-3/2} (Wx)(a,t) \text{,}$$

where the constant C_{ψ} reads:

$$C_{\psi} = \int \left|\omega\right|^{-1} \hat{\psi}(\omega) \text{.}$$

To achieve good time localization, the mother wavelet $\psi(t)$ should decay to zero rather fast, as t reaches the infinity.

In our analysis we have chosen the Morlet wavelet, that is a damped (complex) exponential:

$$\psi(t) = \pi^{-1/4} \exp(-t^2/2 + i\xi_0 t) \text{.}$$

It is well-suited to capture the frequency content of a time series, giving information comparable to that obtained by the Fourier transform methods. Being complex-valued it provides both the modulus measuring the energy density, and the real part commensurate with the intensity and phase of the signal varying in

the time-frequency domain. (In general, wavelet scale is not related to the Fourier wavelength.) The parameter ξ_0 should be large enough (over 5) in order to have a fast decay. By putting $\xi_0 = 2\pi$, beside the fast decay, one also gets the wavelet scale a to be nearly equal to the Fourier wavelength.

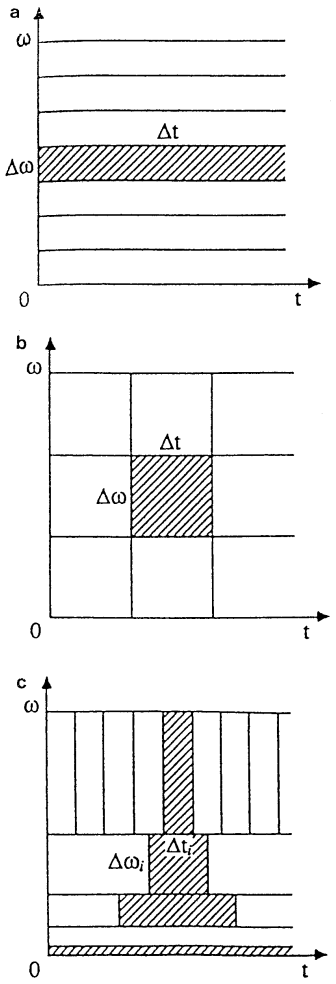

Figure 4. Schematised time-frequency windows used in (a) FFT; (b) WFT; (c) CWT. (modified after Lau and Weng, 1995).

Typically, and we have followed the practice, the CWT is calculated by using the FFT, after sufficient zero padding, to circumvent the periodic nature of the FFT algorithm and obtain a power-of-two data length. Those extra values are removed after the calculation, but the edge effects remain. This is indicated by the so called cone of influence - COI (Torens and Compo, 1998) which is defined using the e-folding value of the wavelet $\psi_{b,a}$, *i.e.* the value t_e at which the

wavelet power $\left|\psi_{b,a}(t_e)\right|^2$ drops to e^{-2}-part of its maximal value. The wavelet spectra values falling outside of the cone of influence should be discarded (or at least taken with care). For the Morlet wavelet, it is convenient to plot absolute values of the real part of the CWT spectra. In this way, one gets a clear view of the spectral intensity and its position in the time-frequency space.

The essential difference between the two analyses is depicted graphically in Figure 4. Also schematized in the figure is the windowed Fourier analysis, discussed in the introduction. One may readily observe the major disadvantage of the Fourier transform when it comes to expanding the non-periodic signals: to compute the transform one has to integrate over all times, obtaining in return the total, non-local spectral amplitudes. Windowing the transform is a move in the right direction, but the WFT window does not have the flexibility of the CWT approach. As it is translated along the time and frequency axes, its width does not change, leaving the shorter-period features under-localized, while over-localizing the features of longer duration.

3. RESULTS AND DISCUSSION

The applied EOF analysis (not discussed in this paper) has allowed the identification of orthogonal spatial patterns in the analysed data set, providing empirical modes subsequently usable as basis functions. It is possible, although not necessary, to interpret thus obtained patterns as the natural modes of variability of the studied field. When the observed Adriatic SST fields were projected onto those functions, the time series representing their variability was obtained. The time series land themselves to further spectral analysis, the results of which are discussed in present section.

The results of the classical Fourier transform analysis of our data are presented in Figure 5. The removal of the temporal mean from the original set (Fig. 5a) has allowed the pattern ranking by temporal variance. In this case, the first EOF mode (not shown) maps the dimensionless, timeless spatial pattern, while the EOF-coefficient time series take care of the observed intra- and inter-annual variability. When the spatial mean is removed instead (Fig. 5c), ranking by spatial variance is allowed. The first EOF mode (not shown) again provides the dimensionless and timeless dominant spatial pattern, and the EOF-coefficient time series picture the variability in time. In both time- and space- detrended series, two components stand out clearly: the annual and semi-annual harmonics. This point is further emphasised in Figures 5b and 5d, in which the signal spectra are plotted after the two harmonics have been removed. The distinct role of these two components is not surprising in the light of the fact that the seasonal cycle

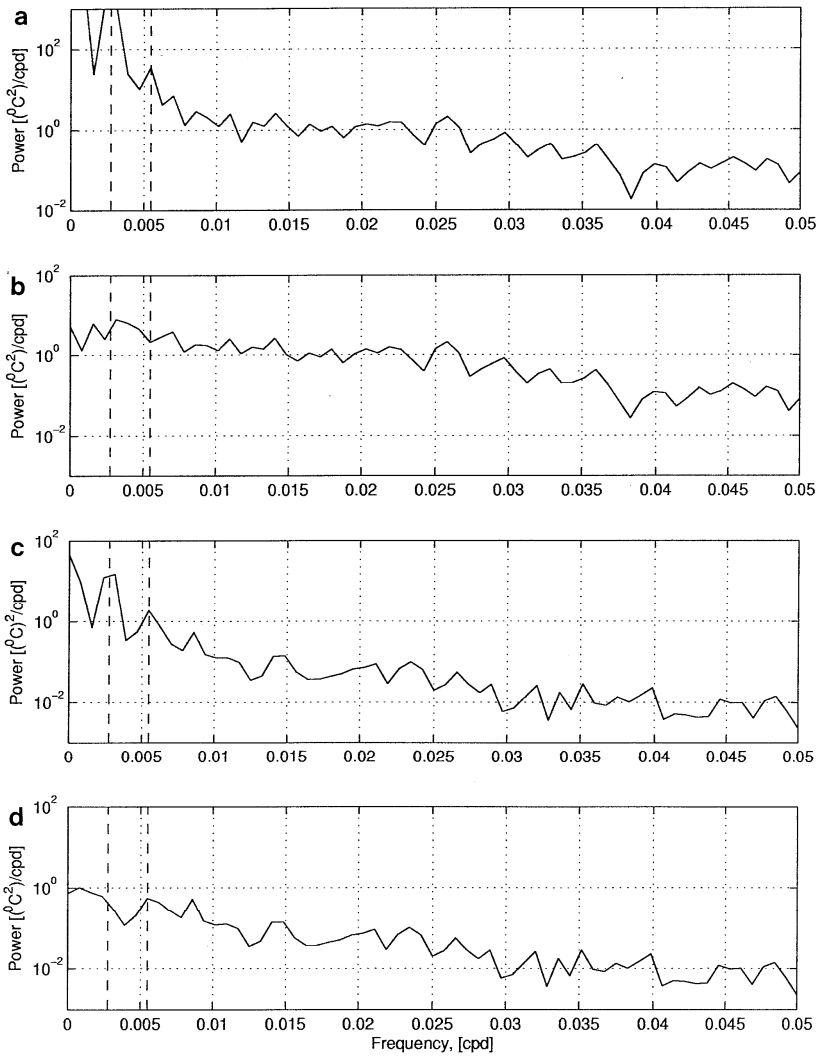

Figure 5. The FFT spectra of the time series depicted in: (a) Fig. 3b (solid line); (b) Fig. 3b (with the annual and semi-annual harmonics removed); (c) Fig. 3c (solid line); (d) Fig. 3c (with the annual and semi-annual harmonics removed). Vertical bars mark the position of the annual and semi-annual harmonic respectively.

physically characterise each year of the Adriatic Sea surface temperature field, and the Fourier integral analysis produces by definition spectral components with a constant amplitude throughout the entire analysed period. In other words, the Fourier transform pinpoints the important natural periodicity, but inevitably imposes on it the assumption of stationarity: the annual and semi-annual harmonics appear in every single year of the 14-year analysed period, each with a constant amplitude. The inter-annual variability is reproduced via interference of higher frequency components, again of constant amplitude. One can say that the Fourier transform offers a global, time-invariant analysis.

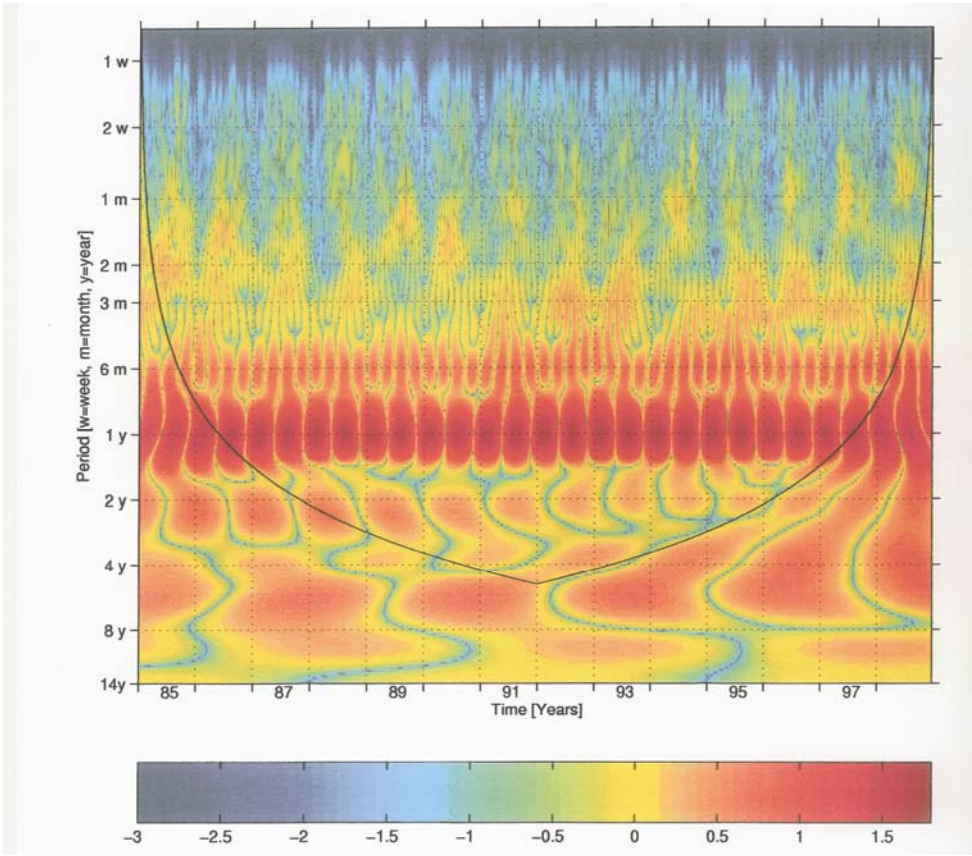

Figure 6a. The CWT spectrum of the time series depicted in Fig. 3b (time demeaned, dominant harmonics included).

In order to catch possible non-stationary, locally transient behaviour in the analysed time series, we made use of the CWT. The results of our CWT analysis (applied to the same EOF-coefficient time series used in the Fourier analysis) are presented in Figure 6 (as before, the time-demeaned signal is analysed first). Also plotted in the figure is the afore-mentioned cone of influence, which maps out the extent of the edge effects. One can readily observe the increased dimensionality of the solution; the absolute value of the real part of the CWT is plotted as a function of the scale (period) as well as the time. In this way, one is able to follow the time-frequency evolution of the analysed signal. Here again, the annual signal dominates the spectrum, but the figure also presents a plenitude of other periodicities, whose intensity changes with time. For example, the removal of the annual and semi-annual harmonics prior to the CWT (not shown) allows not only the bi-annual component to surface, but also the irregularities near the six-month scale to present themselves. As with the FFT, the CWT analysis was performed

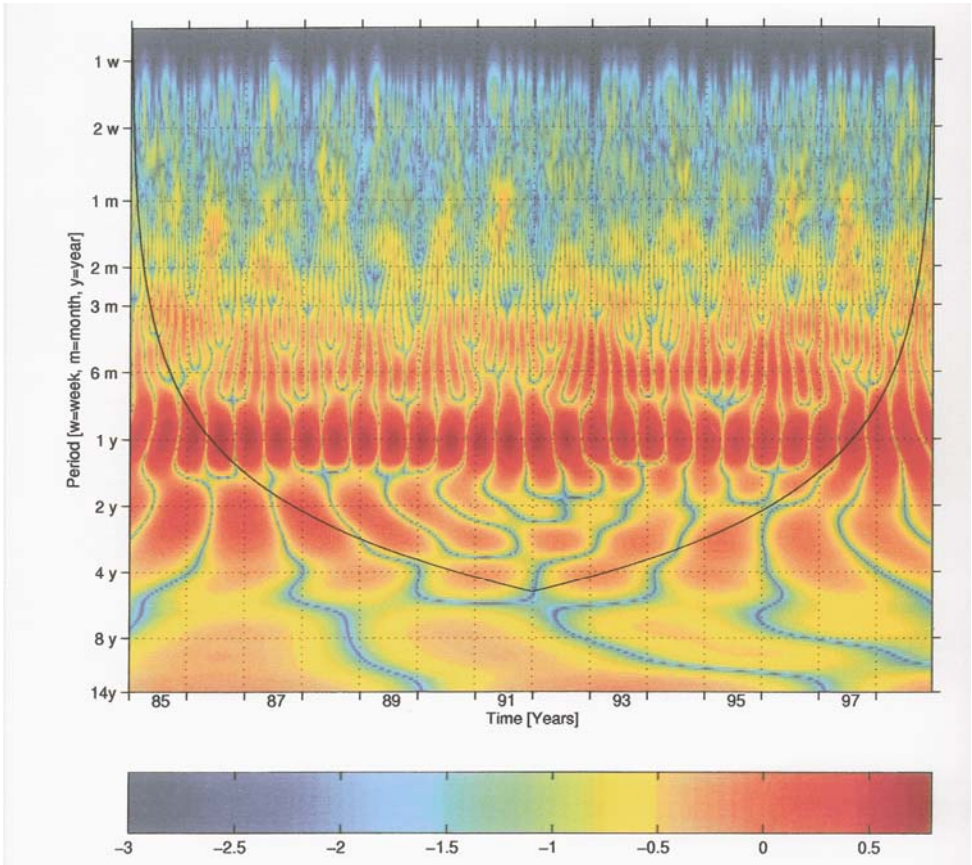

Figure 6b. The CWT spectrum of the time series depicted in Fig. 3c (space demeaned, dominant harmonics included).

on the space-demeaned series, too (Figure 6b). One may readily observe that the seasonal cycle also dominates the spatially demeaned spectrum. Clearly, the variances occur predominantly due to the atmospheric heating and cooling, which are known to exhibit seasonal behaviour. Cross-comparing the outcome of the two techniques (FT and WT), and the two ways the time series were demeaned, one may note that the WT spectra give a clearer indication of the variability at periods other than annual and semi-annual, as well as transient nature of such variability.

Another revealing piece of information is gained by looking at the time series of the wavelet coefficients, band-integrated to discern the dominant/characteristic modes of variability. Figure 7 shows results of such an analysis for the time-demeaned, and Figure 8 for the space demeaned series. In both cases the four bands capture almost 100% variability, as indicated by the error lines practically equal to zero, in the (e) panel on both figures. The top panel (a) in both cases suggests a high-frequency "annual noise" with an occasionally more distinct inter-annual variability, *e.g.* the year 1989 vs. 1993 in case of the time-demeaned

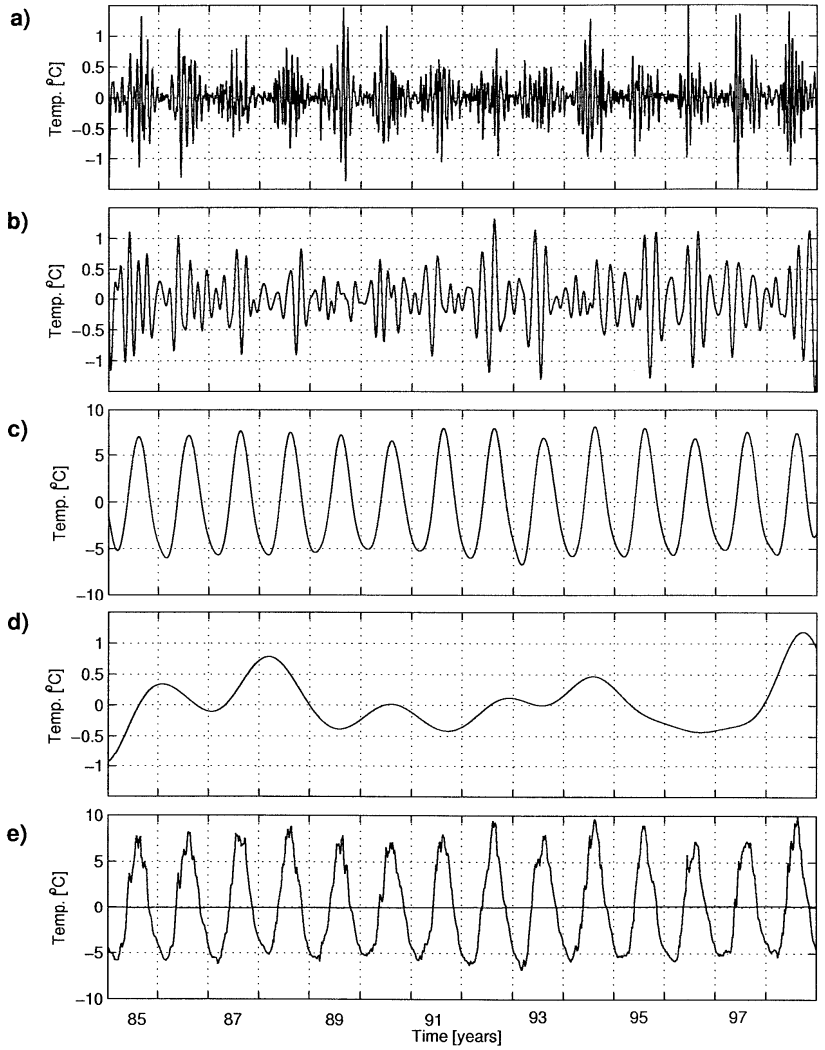

Figure 7. Bend decomposition of the time series CWT analysed in Fig. 6a: (a) 0 –1.5 mo(nths); (b) 1.5 – 4 mo; (c) 4 – 18 mo; (d) 18 – 168 mo; (e) the original time-series band decomposed above – solid line almost identical to zero measures the error of decomposition.

series, or the year 1995 vs. 1996 in case of the space-demeaned data. The intensity of the two signals in this highest frequency band generally reflects the relative relation observed in the original series (panel e): about five times stronger signal remains after time-demeaning than after a prior removal of the spatial mean. Consistent intensity difference is also observed in other bands, in the (semi)annual (4 – 18 months) in particular; here, the size of the time-demeaned amplitude is about an order of magnitude larger than the one for the space demeaned signal. Also, the time-demeaned band exhibits a kind of amplitude modulation throughout the observed period, whereas the space-demeaned band shows more provocative irregularities in the second half of the observed period.

One may conclude that the wavelet analysis offers a much richer view of the analysed data (inter-annual fluctuations in particular), enabling and calling for follow-up oceanographic investigation of the intricacies of the Adriatic Sea surface temperature variability.

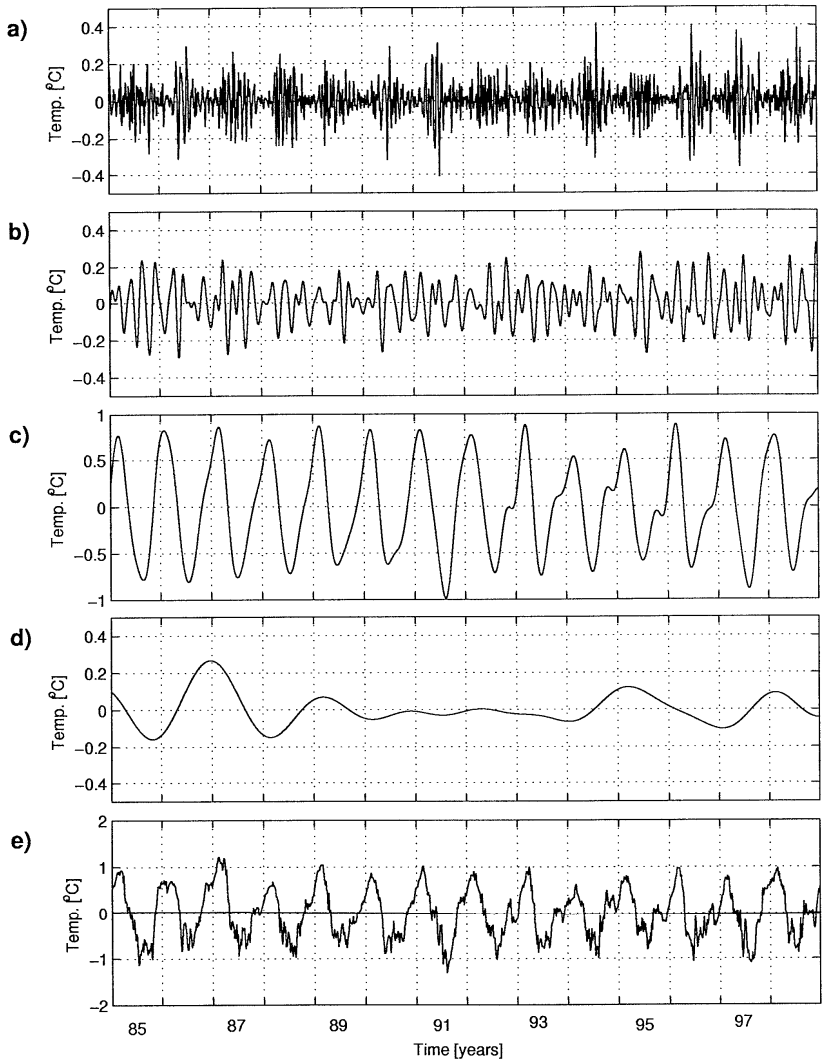

Figure 8. As in Fig. 7, but for the time series CWT analysed in Fig. 6b.

Acknowledgements

Dr. Kenneth Casey kindly provided the NSIPP SST data. The Croatian Ministry of Science, Education and Sports supported this work via research grants 098-0982705-2707 and 119-1193086-3085.

References

1. Bloomfield, P., 2000. Fourier analysis of time series: An introduction. Second Edition. Wiley-Interscience, 288pp.
2. Chui C. K., 1997. Wavelets: A mathematical tools for signal analysis. Society for Industrial and Applied Mathematics, 210pp.
3. Furlan, D., 1977. The climate of southeast Europe. In: Wallen C. C. Ed. Climates of Central and Southern Europe, World Survey of Climatology, Vol. 6, 185-235.
4. Hendershott, M. C. and P. Rizzoli, 1976. The winter circulation of the Adriatic Sea. Deep-Sea Research, 23, 353-370.
5. Kuzmić M. and Z. Pasarić, 2006 Dominant spatio-temporal variability in remotely sensed Adriatic Sea surface temperature. In preparation.
6. Lau K.-M. and H. Wang, 1995. Climate signal detection using wavelet transform: How to make a time series sing. Bulletin of the Meteorological Society, 76, 2391-2402.
7. Raicich F., 1994. Note on the flow rates of the Adriatic rivers. CNR, Istituto Talassografico Technical report RF 02/94, 8pp.
8. Torens S., and G. P. Compo, 1998. A practical guide to wavelet analysis. Bulletin of the American Meteorological Society, 79, 61-78.